

Enantioselective Epoxidation of Electrophilic Olefins by Using Glycosyl Hydroperoxides

Wioletta Kośnik,^[a] Wojciech Bocian,^[a] Lech Kozerski,^[a] Igor Tvaroška,^[b] and Marek Chmielewski*^[a]

Abstract: Anomeric hydroperoxides derived from 3,4,6-tri-*O*-benzyl-galactose and glucose were used for enantioselective epoxidation of naphthoquinone (**12**), chalcone (**13**), (*E*)-1,2-dibenzoyl ethylene (**14**) and (*E*)-*iso*-butyryl-phenyl ethylene (**15**). In the presence of sodium hydroxide, the epoxidations showed exceptional high

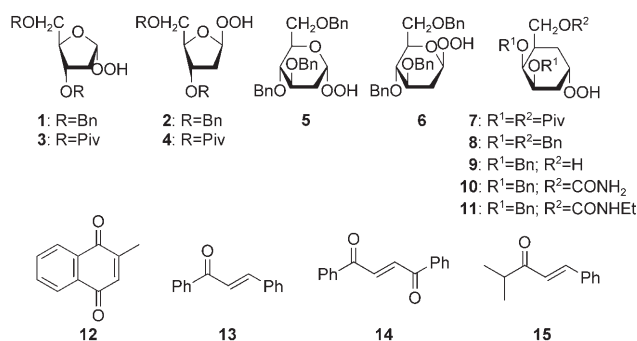
asymmetric induction. The exchange of sodium by a potassium ion resulted in a low asymmetric induction. These re-

Keywords: anomeric oxidation • asymmetric synthesis • density functional calculations • epoxidation • hydroperoxides

sults pointed to the crucial role of the counterion and strongly suggested that coordination of the alkaline ion occurs in the transition state of the epoxidation process by both reagents, hydroperoxide and the olefin. Theoretical studies of the reaction mechanism at the DFT B3LYP/6-31G* level fitted very well with experimental results.

Introduction

We have recently reported our results on the anomeric hydroperoxides **1–8**, which can be obtained from the respec-

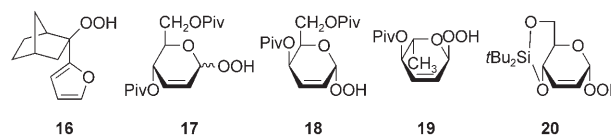


tive 3,5-di-substituted-2-deoxy-D-erythropentofuranose, 3,4,6-tri-*O*-substituted-2-deoxy D-arabino, and D-lyxohexopyranoses, or their corresponding glycosides by treatment with hydrogen peroxide in the presence of an acid catalyst.^[1] Hydroperoxides **1–8** are relatively stable, can be separated into pure anomers by column chromatography, and stored in the refrigerator without visible decomposition.^[1] Hydroperoxides, thus obtained, were used for the base-catalyzed enantioselective epoxidation of 2-methyl-1,4-naphthoquinone (**12**) to give, however, only moderate enantioselectivities, *ee* values (*ee* = enantiomeric excess), of about 28–47%.^[1] A similar enantioselectivity, for the same olefin with 1-phenylethyl-hydroperoxide, has been reported by Adam et al.,^[2] by Lattanzi et al.^[3] for the asymmetric epoxidation by using hydroperoxides derived from the (+)-norcamphor derivatives **16**, and by Taylor et al.^[4] for epoxidations by using anomeric hydroperoxides derived from the 4,6-disubstituted-2,3-unsaturated pyranoses **17–20**.

[a] W. Kośnik, Dr. W. Bocian, Prof. Dr. L. Kozerski, Prof. Dr. M. Chmielewski
Institute of Organic Chemistry of the Polish Academy of Sciences
Kasprzaka 44/52, 01–224 Warsaw (Poland)
Fax: (+48) 22-6326681
E-mail: chmiel@icho.edu.pl

[b] Dr. I. Tvaroška
Institute of Chemistry of the Slovak Academy of Sciences
Dubravská cesta 9, 845 38 Bratislava (Slovakia)

Supporting information for this article is available on the WWW under <http://www.chemurj.org/> or from the author.



The syntheses and properties of these and other organic peroxides have recently been reported.^[5]

The particular aim of our investigation was to find a sugar, which, after oxidation of the anomeric center, would

provide exclusively or almost exclusively only one hydroperoxide (α - or β -anomer). This could enable a possible reuse of the reagent. It should be pointed out that the initial proportion of α - and β -anomers of sugar hemiacetal does not necessarily control the proportion of derived anomeric hydroperoxides, since the hydroperoxide group has been shown to exhibit a stronger anomeric effect than the hydroxyl group.^[6] The possibility of recovery of hemiacetal and its subsequent reoxidation to the hydroperoxide would enhance significantly the overall economy of this process. On close examination of the representative group of 2-deoxy-sugars, it was found that the derivatives of 2-deoxy-galactose react to give the corresponding hydroperoxides **7–11**, which contain only about 6–7% of the β -anomer. Therefore, the readily available hydroperoxide **8** could be used for the epoxidation without prior separation of the minor β -anomer.

To examine the influence of a substitution at the C-6 carbon atom of a sugar on the direction and magnitude of enantioselectivity of epoxidation, we also used three additional hydroperoxides **9**, **10**, and **11**, in addition to **8**, which were all synthesized in a similar manner. To compare the results of epoxidation by α - and β -anomers, the anomeric hydroperoxides (**5** and **6**), derived from 3,4,6-tri-*O*-benzyl-2-deoxy-glucose, were separated and used independently. To compare our stereoselectivity results with those reported in other laboratories, four electrophilic olefins were selected: the quinone **12**, chalcone (**13**), (*E*)-1,2-dibenzoyl ethylene (**14**) and (*E*)-*iso*-butyryl-phenyl, ethylene (**15**). The aim of this investigation was to find not only the optimal conditions, but also to suggest a plausible rationale of the stereochemical pathway of the epoxidation.

Preliminary results of epoxidation of the quinone **12** with hydroperoxides **1–8** prompted us to examine the influence of other base catalysts, in particular, inorganic bases. To rationalize the direction and magnitude of the asymmetric induction observed during the epoxidation of chalcones we decided to carry out the quantum-mechanical calculations of possible reaction pathways to determine the most probable structure for a transition states for this reaction.

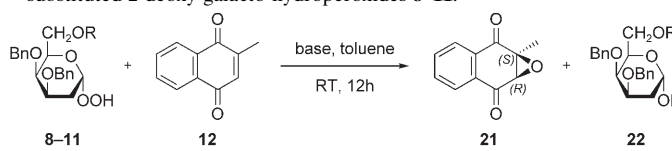
Results and Discussion

Epoxidation reactions: The epoxidation was carried out by following procedures reported earlier by us^[1] and Taylor's laboratory.^[4a] The diastereo-purity of hydroperoxides and proportions of enantiomeric epoxides were assigned by the HPLC. All enantioselective epoxidations were repeated by using independently synthesized hydroperoxides, to guarantee reliable and reproducible results. In the case of epoxidations that were performed in the presence of sodium or potassium hydroxide, one to four hours were required to complete the reaction and the product was obtained in 92–98% yield. On the other hand, the epoxidations performed in the presence of DBU (DBU = 1,8-diazabicyclo[5.4.0]undec-7-ene) took 1–7 days to complete and afforded the product in a good 92% yield for the quinone **12**; for en-ones **13** and **14**

the products were formed in poor 27–38% yields and the en-one **15** did not react.

The epoxidation of **13** by the readily available hydroperoxide **8** was also performed in the presence of other bases. Hence, in the presence of lithium hydroxide hydrate or the anhydrous reagent, the reaction provided the corresponding epoxides in 95–96% yields and were completed within three and six days, respectively. A similar high yield was observed for the same epoxidation in the presence of cesium hydroxide hydrate, but the reaction was as fast as that in the presence of sodium or potassium hydroxide. The en-on **13** can be epoxidized also in the presence of tetramethyl ammonium hydroxide hydrate to afford the epoxide after one hour in 78% yield. The results of all the reactions performed and the relevant enantioselectivity data are presented in Tables 1 and 2.

Table 1. Experimental data for the epoxidation of **12** by α -anomers of 6-substituted 2-deoxy-galacto-hydroperoxides **8–11**.



Hydroperoxide	Base	ee [%] ^[a]
8 : R = Bn (7% of β , HPLC)	DBU	43
	KOH·H ₂ O	42
	NaOH	40
9 : R = H (7% of β , HPLC)	DBU	53
	KOH·H ₂ O	39
	NaOH	25
10 : R = CONH ₂ (8% of β , HPLC)	DBU	55
11 : R = CONHEt (3% of β , HPLC)	DBU	51

[a] Determined by HPLC.

The enantioselectivity of the epoxidation of the quinone **12** with hydroperoxides **8–11** to afford the epoxide **21** did not depend on the base used (Table 1). The hydroperoxides with more polar groups at the C-6 carbon atom, such as **9** and **10**, gave epoxides with only marginally better selectivities. The results are similar to those reported by Taylor et al.^[4] for the epoxidations by using 2,3-unsaturated anomeric hydroperoxides **17–20** and by Lattanzi et al.^[3] for the hydroperoxide **16** related to the furyl-bornane system.

It should be pointed out that the recovery of pure hemiacetal **22** after epoxidation was as high as 80%. This observation is in contrast to the epoxidation of olefins by using 2,3-unsaturated anomeric hydroperoxides **17–20**.^[4,7] In the latter case, likely due to the low stability, the recovery of corresponding unsaturated hemiacetals could not be achieved.^[8]

Significantly different results were observed for the epoxidation of **13**, dibenzoyl ethylene **14**, and butyryl-phenyl ethylene **15** (Table 2) with hydroperoxides **8**. The enantioselectivity of the epoxidation led to formation of **23**, **24**, and **25**,

Table 2. Experimental data for the epoxidation of en-ones **23–25** by hydroperoxides **8**, **5**, and **6**.

8: R₁=OBn, R₂=R₃=H, R₄=OOH

5: R₁=R₃=H, R₂=OBn, R₄=OOH

6: R₁=R₄=H, R₂=OBn, R₃=OOH

13: R₁=R₂=Ph

14: R₁=Ph, R₂=COPh

15: R₁=iPr, R₂=Ph

23: R₁=R₂=Ph

24: R₁=Ph, R₂=COPh

25: R₁=iPr, R₂=Ph

23

24

25

ent-**23**

Reaction	Conditions	<i>ee</i> [%] (configuration) ^[a]
8 + $\xrightarrow[\text{toluene, RT}]{\text{base}}$	KOH·H ₂ O	11 (2 <i>R</i> ,3 <i>S</i>)
	NaOH	90 (2 <i>S</i> ,3 <i>R</i>)
	LiOH·H ₂ O	32 (2 <i>S</i> ,3 <i>R</i>)
	LiOH	5 (2 <i>S</i> ,3 <i>R</i>)
	CsOH·H ₂ O	20 (2 <i>R</i> ,3 <i>S</i>)
	DBU	39 (2 <i>S</i> ,3 <i>R</i>)
	Me ₄ NOH·5 H ₂ O	13 (2 <i>S</i> ,3 <i>R</i>)
8 + $\xrightarrow[\text{toluene, RT}]{\text{base}}$	KOH·H ₂ O	12 (2 <i>S</i> ,3 <i>S</i>)
	NaOH	78 (2 <i>S</i> ,3 <i>S</i>)
	DBU	6 (2 <i>S</i> ,3 <i>S</i>)
8 + $\xrightarrow[\text{toluene, RT}]{\text{base}}$	KOH·H ₂ O	10 (2 <i>S</i> ,3 <i>R</i>)
	NaOH	85 (2 <i>S</i> ,3 <i>R</i>)
	DBU	does not react
5 + $\xrightarrow[\text{toluene, RT}]{\text{base}}$	KOH·H ₂ O	8 (2 <i>S</i> ,3 <i>R</i>)
	NaOH	95 (2 <i>S</i> ,3 <i>R</i>)
	DBU	61 (2 <i>S</i> ,3 <i>R</i>)
6 + $\xrightarrow[\text{toluene, RT}]{\text{base}}$	KOH·H ₂ O	54 (2 <i>R</i> ,3 <i>S</i>)
	NaOH	80 (2 <i>R</i> ,3 <i>S</i>)
	DBU	58 (2 <i>R</i> ,3 <i>S</i>)

[a] Determined by HPLC.

respectively, depending on the base used. Whereas for DBU and lithium hydroxide hydrate, the *ee* values of **23** were similar to those observed previously, in the presence of sodium and potassium hydroxide, the results were dramatically different. Sodium hydroxide yielded a very high asymmetric induction, 90% *ee*, whereas with the potassium hydroxide, only a low induction in the opposite direction, 11% *ee*, was found. The latter result is similar to that reported by Adam's group (14%).^[24] Cesium hydroxide hydrate as a catalyst of epoxidation of **13** by hydroperoxide **8** provided **23** with 20% *ee*, similar in value and in the same direction of induction as were noticed for potassium hydroxide. In the case of epoxidation of **14** catalyzed by DBU, the enantioselectivity was low, whereas en-one **15** in the presence of the same base did not react at all. An interesting result was obtained for the epoxidation of **13** by **8** in the presence of lithium hydroxide, the monohydrate provided an *ee* value in the range observed for DBU, whereas the anhydrous base gave a very low asymmetric induction, 5% *ee*.

High asymmetric induction was observed also for the epoxidation of **14** by **8** in the presence of sodium as a counterion (78% *ee*). The exchange of sodium by a potassium ion resulted in a low asymmetric induction (12% *ee*) in the

same direction as for the sodium ion. A similar result was noticed for the epoxidation of en-one **15**. Hydroperoxide **8** in the presence of the sodium ion gave the product with 85% *ee*, whereas in the presence of potassium, the epoxide **25** was formed with only 10% *ee* and with the same direction of induction as for the sodium ion.

It is worth noting that the hydroperoxide **8** contains 5–7% of the β -anomer, which obviously produces the opposite direction of asymmetric induction. It means that the real induction for the epoxidation of **13** by **8** in the presence of sodium hydroxide should reach 95% *ee*. This was exemplified when epoxidation of the **13** with pure α - (**5**) and β -anomer (**6**) was performed (Table 2). Hydroperoxide **5** with chalcone **13** in the presence of sodium hydroxide afforded **23** with 95% *ee*, whereas β -anomer **6** gave the corresponding *ent*-**23** with 80% *ee*. The addition of [15]crown-5 ether to the reaction mixture of **8** and **13**, to disrupt the formation of the hydroperoxide/sodium ion complex, diminished induction to the level of 46% *ee*. In the case of the same reactants and potassium hydroxide, addition of [18]crown-6 did not change induction significantly (9% *ee*). These results pointed to the crucial role of the counterion and strongly suggested the coordination of the alkaline metal ion in the transi-

tion state of the epoxidation process by both reagents, hydroperoxide, which includes sugar oxygen atoms, and the olefin. It should also be mentioned here that the commercially available sodium (anhydrous) and potassium (15% water) hydroxides were used for the epoxidation of olefins. The content of water was not discussed as a determining factor that might influence the stereochemical pathway of the epoxidation. Although the example of lithium hydroxide, anhydrous and monohydrate, showed that the content of water may influence the reaction rate and the enantioselectivity, comparison of the anhydrous lithium and sodium hydroxide testify, however, that the counter ion is the crucial factor in the reaction and not the presence of a water. For this reason, the water was not included explicitly in our calculations because in the case of glycosyl hydroperoxides, the metal cations are exhaustively coordinated by sugar oxygen atoms (vide infra). This situation is, therefore, quite different from the epoxidations carried out with the alkylaryl hydroperoxides.^[2c,d] The significantly different enantioselectivity observed for quinone **12** and open-chained en-ones **13**, **14**, and **15** strongly implies that the *s-cis* conformation of the en-one fragment in the transition state is the critical factor, which allows for the effective coordination of the central metal cation and consequently leads to the high asymmetric induction observed. It is known that en-ones with rigid *s-cis* conformations are epoxidized with high asymmetric induction.^[9] Such *s-cis* geometry of the en-one has also been postulated to explain the stereochemical pathway of the epoxidation.^[2,10]

Conformation of the hydroperoxide group and its anion:

The relatively uniform ¹H NMR spectroscopic chemical shift ($\delta = 9\text{--}10$ ppm) for the hydroperoxide proton of all α and β anomeric hydroperoxides **5–11**,^[1,11] may suggest the presence of a hydrogen bond between hydroperoxide proton and the ring oxygen atom in solution (Figure 1). This pre-

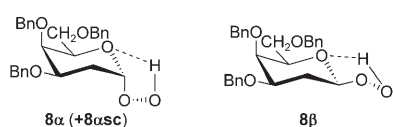


Figure 1. Preferred structures of both α and β anomers of hydroperoxide **8**.

ferred geometry is supported by quantum mechanical calculations. Thus, by using the nomenclature of the anion peroxide shown in Figure 2, the hydroperoxide conformation **+8asc** is 3.77 and 4.08 kcal mol⁻¹ lower in energy than **-8asc** and **8cap**, respectively, as calculated by DFT B3LYP/6-31G(d,p).

The glycosyl peroxide anion can adopt three conformations as shown in Figure 2. For **8 α** , the **-sc** conformation is the most stable. The next most stable conformer is the **8cap** orientation with the energy at 3.08 kcal mol⁻¹ higher than **-8asc**, as calculated at the DFT (B3LYP/6-31++G(d,p))//

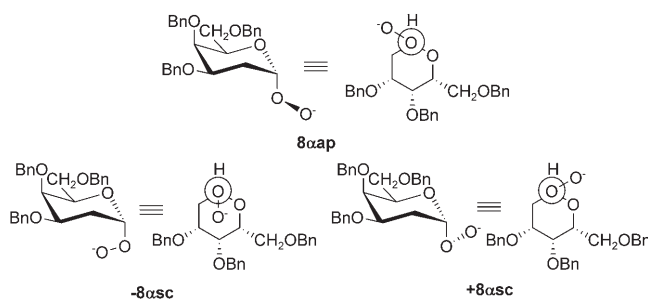


Figure 2. The three rotamers of the α -anomer of hydroperoxide anion, **8cap**, **-8asc**, and **+8asc**, respectively.

B3LYP/6-31G(d,p) level. The energy of the **+8asc** conformer is 3.68 kcal mol⁻¹ higher than **-8asc**.

One can discuss the role of these conformations in the enantioselective epoxidation. The lowest energy conformation **-8asc** could be assumed to be a part of the transition state of enantioselective epoxidation, especially in the case of DBU as a base catalyst. Whereas the less sterically accessible **-sc** conformation may create better steric conditions for the discrimination of enantiofaces of a substrate, there is free access from both enantiofaces of chalcone in the case of the **8cap** and **+8asc** conformations and, therefore, they are less effective in producing stereoselection. It would be difficult, however, to explain the high asymmetric induction on the basis of this conformation alone, since the exact locations of both reagents and the base are not well defined. On the other hand, the highest-energy conformation **+8asc** of the free anion is the most likely conformation for a chelation of the metal cation, in which the metal is coordinated by both the ring oxygen and the terminal benzyloxy group.

The close similarity of the asymmetric induction in the epoxidation of **13** by 2-deoxy-galactose hydroperoxide **8** and 2-deoxy-glucose congener **5** in the presence of sodium hydroxide implies that oxygen atoms of benzyloxy groups at C-3 and C-4 do not participate in the coordination of the metal ions. Bearing that in mind, one can hypothesize that the hydroperoxide proton and the alkaline ion in the hydroperoxide alkaline salt have the same location with respect to the sugar. Consequently, it is obvious that, in contrast to the sodium ion, the potassium ion with a larger atomic radius generates more steric congestion and thus is enlarging the distance between reacting sites (Figure 3).

Nevertheless, to establish the location of the metal cation, the equilibrium molecular geometry calculations of the corresponding complexes were carried out. In these calculations, the benzyl groups were replaced with methyl groups to shorten the computational time. The calculated Na⁺ complexes with **26** at the DFT (B3LYP/6-31++G(d,p)) level are shown in Figure 4. As expected, the lowest-energy complex is **26a** with the **+sc** about the C-O1 linkage. The energies of complexes **26b–e** are 2.96, 14.25, 31.01, 50.85 kcal mol⁻¹ higher than for **26a**, respectively. The complexation energy of **26a** is 156.6 kcal mol⁻¹.

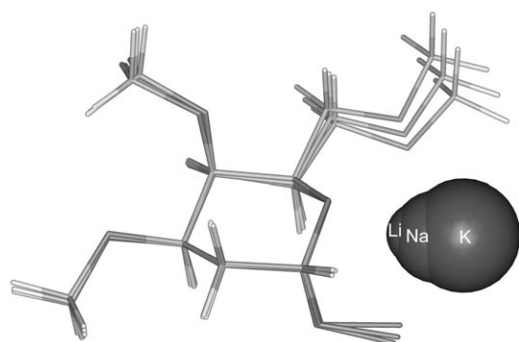


Figure 3. Superposition of glycosyl peroxide complexed with different cations of 3,4,6-tri-*O*-methyl-2-deoxy- α -D-lyxohexopyranosyl hydroperoxide (**26**). The geometries were calculated at the DFT (B3LYP/6-31++G(d,p)) level.

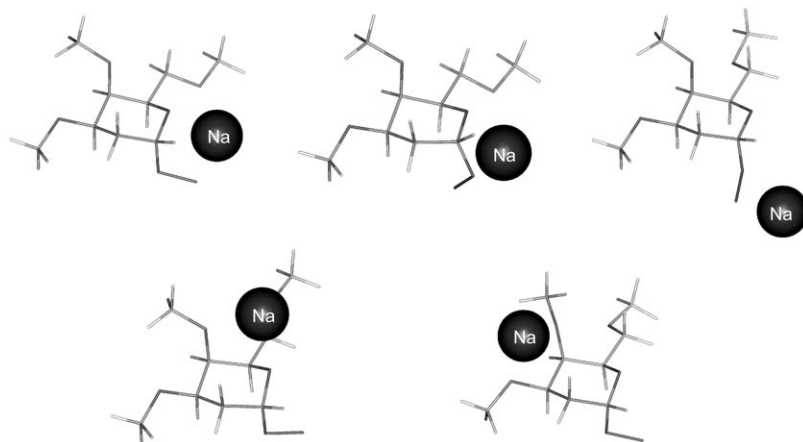


Figure 4. Predicted geometries of sodium cation complexed peroxides **26**.

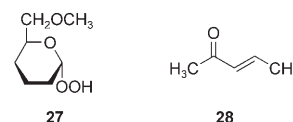
It is evident that the energy of a complex depends on the number of oxygen atoms involved in the coordination of the cation. Four oxygen atoms coordinate the metal in the **26a** and **26b** complexes and, as a consequence, their energy is lower relative to the **26c**, **26d**, and **26e** complexes. This implies that for the epoxidation reaction in the presence of a metal cation, only the **26a** and **26b** complexes should be considered as reactant structures. However, the unfavorable conformation of the peroxide oxygen creates a steric hindrance to an attack of a chalcone in the case of **26b**. Therefore, in our study, the **26a** complex was assumed.

Mechanism of the enantioselective epoxidation: The debate on the clarification of the molecular-oxygen-transfer mechanism in electrophilic double-bond epoxidation reactions has continued for more than three decades.^[12–15] Despite of spectacular achievements of catalytic asymmetric epoxidation of allylic alcohols by Sharpless^[16] or *Z* alkenes by Jacobsen,^[17] the main issue concerns the stepwise^[18] versus concerted^[16] addition of oxygen to a double bond. On the other hand, the epoxidation of α,β -unsaturated ketones with peroxides under basic conditions has been known for decades to proceed in a stepwise manner.^[19] Nevertheless, the enantioselectivity

of the nucleophilic epoxidation reaction still remains a challenge in chemical synthesis.^[5,9,10,20] To address this problem in the present work, we have carried out the theoretical studies of the reaction mechanism at the DFT level by means of the free energies of the transition states and inclusion of solvent effects. To shorten the computational time, we have used the modified 2,3,4-trideoxy-6-*O*-methyl- α -D-glycero-hexopyranosyl peroxide. This modification has no effect on a stereoselection since we have shown that only oxygen atoms shown in **27** have an influence on the cation binding (see Figure 4 and the discussion above). On the other hand, the experiment shows that substituents present in the α,β -unsaturated ketone play a decisive role in the steric course of the reaction. Therefore, to see if this is reflected in our computations, we have used **13** and (*E*)-pent-3-en-2-one (**28**)[†].

We have restricted our calculations to the α -anomer of hydroperoxide since its significance is much higher than that of the β -congener, which is always a minor component of a mixture after anomeric oxidation and requires chromatographic separation.

Two distances were used as reaction coordinates to follow the reaction mechanism of the enantioselective epoxidation of electrophilic olefins by using glycosyl hydroperoxides (Figure 5): the distance $r(\text{O}2-$



C3) between the peroxy oxygen of the glycosyl peroxide and the carbon atom of the olefin and the distance $r(\text{O}2-\text{C}2)$ between the peroxy oxygen of the glycosyl peroxide and the second carbon atom of the olefin. These geometrical parameters reflect the nucleophilic attack of the peroxy oxygen atom and formation of an epoxide. Two cations, namely, sodium and potassium, for complexes and two different reactant orientations representing two different enantiomeric pathways were assumed in calculations that led to four geometries of a reaction complex (two for the sodium cation and two for the potassium cation; Figure 5). Reaction

[†] Following the IUPAC rules of nomenclature, the numbering of the carbon atoms in chalcones and pent-3-en-2-one is not the same, that is, carbon atoms C-2 and C-3 of the former molecule refer to C-3 and C-4 of the latter. To relate the calculations to the experimental results we have used the numbering valid for the chalcone molecule, which was used in the experiment

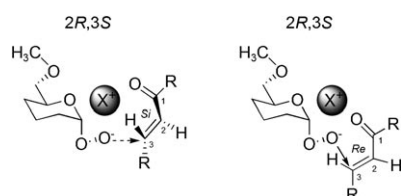


Figure 5. Two enantiomeric pathways of the carbohydrate metal complex and the *s-cis* en-one molecule; R = Ph, Me.

mechanisms for two stereoselective models were followed by means of the two-dimensional energy maps calculated as a function of the predefined above reaction coordinates (Tables 3 and 4).

The potential energy surface calculated at the B3LYP/6-31G* level for the reaction mechanism of the sodium that leads to the 2*S*,3*R* product is represented in the form of a two-dimensional reaction coordinate contour diagram, as shown in Figure 6. The distances plotted along both axes of the contour map describe nucleophilic attack of the peroxy oxygen O-2 on the first olefinic carbon C-3 (horizontal axis) and the closing of the epoxide ring with the second olefinic carbon (vertical axis). A reaction pathway is readily identified on this potential energy surface. The potential energy surface shows one intermediate (★) and two energy barriers (✕). Very similar surfaces were calculated for the other three models. Thus, the reaction must proceed through a stepwise mechanism from reactants (▲) to the product complex (▲).

The relative free energies of the optimized stationary points for the different models are given in Table 3 and selected geometrical parameters are given in Table 4. The free energy was calculated as a sum of the electronic energy calculated at the B3LYP/6-311+G** level with solvent effects of toluene calculated by using the IEF-PCM model, and the thermal free energy correction term for 298.15 K calculated at the B3LYP/6-31+G* level by using frequency correction factor = 0.963. All geometries were calculated at B3LYP/6-31G* level.

The structures of transition states for the reaction of a sodium complex of **27** with **13** are presented in Figure 7.

Table 4. Selected DFT calculated distances in the stationary points observed on potential energy surfaces of two models described in Figure 5 at the B3LYP/6-31G* level for **13**.

Complex	Complex	Selected distances [Å]		
		O2–C3	O2–C2	O1–O2
2 <i>R</i> ,3 <i>S</i> with sodium	TS1	2.839	2.868	1.481
	intermediate complex	1.489	2.332	1.514
	TS2	1.424	2.100	1.788
2 <i>S</i> ,3 <i>R</i> with sodium	product complex	1.455	1.425	3.384
	TS1	2.447	3.100	1.477
	intermediate complex	1.471	2.291	1.560
2 <i>R</i> ,3 <i>S</i> with potassium	TS2	1.436	2.179	1.684
	products complex	1.457	1.425	3.444
	TS1	2.498	3.125	1.458
2 <i>R</i> ,3 <i>S</i> with potassium	intermediate complex	1.482	2.347	1.502
	TS2	1.408	2.038	1.857
	product complex	1.459	1.424	3.669
2 <i>S</i> ,3 <i>R</i> with potassium	TS1	2.500	3.264	1.484
	intermediate complex	1.471	2.321	1.533
	TS2	1.430	2.166	1.692
2 <i>S</i> ,3 <i>R</i> with potassium	product complex	1.455	1.423	3.608

The corresponding transition-state structures for analogous potassium complexes are similar and are presented in the Supporting Information. This also concerns the computational data and respective figures for the reaction of **27** with **28**. The comparison of sodium and potassium geometries revealed only a subtle difference. The structures shown in Figure 7 illustrate differences in the transition-state geometry for pathways leading to the different stereochemical products. The transition-state **TS1** for the nucleophilic attack occurs as the first step in the reaction and the O2–C3 distance has values of 2.84 and 2.45 Å, respectively. **TS1** leading to the 3*S* configuration shows the orthogonal orientation of the planes defined by the C1–O1–O2 angle of the sugar and the chalcone molecule, whereas their parallel orientation leads to the enantiomer with the 3*R* configuration. In the second reaction step, the transition-state **TS2** represents the formation of the O2–C2 bond. The O2–C2 bond length has values of 1.42 and 1.44 Å for the 2*R* and 2*S* configurations, respectively.

Table 3. Comparison of the DFT relative free energies [kcal mol⁻¹] with included solvent effects of toluene (IEF-PCM), calculated for the stationary points observed on potential energy surfaces in two models described in Figure 5 for **13**. Also included are imaginary frequencies of all transition states. The corresponding data with no solvent effects is shown in brackets.

Complex	Free energy ^[a]			
	Na		K	
	2 <i>R</i> ,3 <i>S</i>	2 <i>S</i> ,3 <i>R</i>	2 <i>R</i> ,3 <i>S</i>	2 <i>S</i> ,3 <i>R</i>
separated substrates	–873334.064 ^[b] (–873324.458) ^[b]		–1147951.829 ^[b] (–1147942.205) ^[b]	
TS1	15.02 (1.94)	13.08 (0.23)	13.17 (1.91)	13.71 (1.60)
intermediate complex	7.88 (–4.28)	5.50 (–5.86)	5.52 (–4.67)	7.67 (–2.97)
TS2	10.11 (–3.13)	6.93 (–5.41)	8.55 (–2.68)	8.20 (–2.91)
products complex	–27.38 (–42.15)	–29.03 (–43.06)	–27.00 (–40.32)	–29.37 (–41.75)
imaginary freq. TS1 [cm ⁻¹]	(–32.2)	(–32.6)	(–40.7)	(–40.0)
imaginary freq. TS2 [cm ⁻¹]	(–176.6)	(–117.6)	(–181.8)	(–129.7)

[a] Electronic energies calculated at the B3LYP/6-311+G** level, frequencies and free energy corrections calculated at the B3LYP/6-31+G* level, frequency correction factor = 0.963. [b] The absolute free energy.

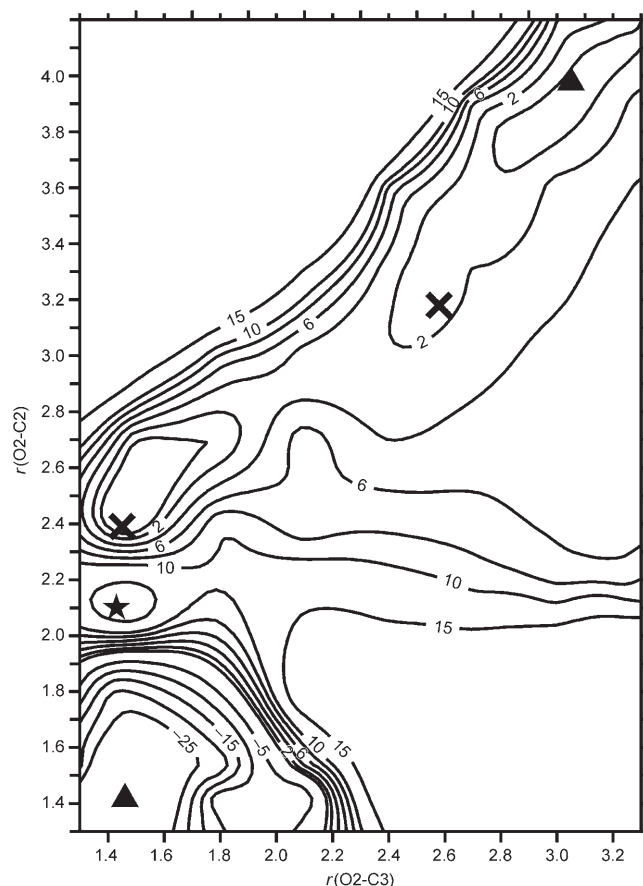


Figure 6. Potential energy surface calculated at the B3LYP/6-31G* level and corresponding to the stepwise mechanism in the reaction of **27** and **28**. The numbers in italics represent relative energies [kcal mol⁻¹] with respect to the reactant complex. x represents transition states, ★ represents an intermediate, and ▲ represents both the reactant and product complex.

The information from the calculated potential energy surfaces facilitated the rationalization of divergence of reaction pathways for the sodium and potassium cations complexes that experimentally lead the reactions in the opposite direction of asymmetric induction (they are presented in Figure 8). In the case of sodium complexes, the free energy of the 2*S*,3*R* enantiomer is lower (Figure 8 in red, Table 3) for both transition states and for the substrates and respective products. The calculated free energy difference between the pathways for the two enantiomers is quite large and thus may explain the formation of the major product observed experimentally between **8** and **13** (2*S*,3*R*) (Table 2).

The interpretation of stereoselection for the potassium ion complexes is well explained if the influence of the solvent is included in the calculations. The experiment yields a slight excess of the reverse configuration, 2*R*,3*S*, whereas the free-energy calculations for both transition states are lower for the opposite configuration (as found in sodium complexes) without consideration of a solvent. If the solvent is considered in the calculations, they reflect the experiment properly, except for the reverse energy levels for the second

transition state. But the relative energy of a barrier leading to the more important first transition state,^[20] that is, **TS1**, is lower and therefore, in agreement with the configuration found experimentally.

The computational data for the reaction of **27** with **28** shows that the difference in the energy barrier of the first transition state leading to the stereoselection is much smaller (see the Supporting Information). Therefore, on the basis of these calculations, one may expect a worse stereoselection upon experiment. It should be pointed out that only in the case of **13**, the direction of asymmetric induction for sodium and potassium counterions is opposite. For the **14** and **15**, the counterion does not change the direction of induction, and only its magnitude for the potassium cation is significantly lower. Moreover, the peroxide **27** used as model for calculations does not necessarily reflect the reagent used, **8**.

Conclusion

It has been shown that anomeric hydroperoxides can be used as effective reagents for the enantioselective epoxidation of electrophilic olefins in the presence of bases. Particularly attractive is readily available hydroperoxide **8** derived from perbenzylated 2-deoxy-galactose because it exists as an almost pure α -anomer and can be used for the epoxidation without prior separation of the minor β -anomer. Moreover, the hemiacetal **22** can be easily recovered after epoxidation and reoxidized to the hydroperoxide **8**. This significantly enhances the economy of the whole process.

A remarkable role is played by the sodium counterion and by the *s-cis* conformation of the en-one molecule in these reactions, which allow for the temporary formation of a highly organized reaction complex and consequently lead to the enhanced stereoselection. The role of the counterion coordination by both reagents during the epoxidation reaction has been observed for the first time and was well explained by the quantum-molecular calculations of the stereochemical pathway for this two-steps process.

Experimental Section

General information: Melting points were determined on a Koeffler hot-stage apparatus. NMR spectra were recorded by using Bruker Avance 500 instruments (absorptions of aromatic protons and carbon atoms were not reported). IR spectra were recorded on a Perkin-Elmer FTIR Spectrum 200 spectrophotometer. UV spectra were measured on a Cary 100 spectrophotometer in acetonitrile and isopropyl alcohol. CD spectra were recorded between 180 and 400 nm at room temperature with a JASCO J-715 spectropolarimeter by using acetonitrile and isopropyl alcohol solutions. Solutions with concentrations in the range of 0.8×10^{-4} to 1.2×10^{-3} mol dm⁻³ were examined in cells with a path length 0.1 or 1 cm. Mass spectra were recorded by using AMD-604 Inectra GmbH and HPLC-MS with Mariner and API 356 detectors. Optical rotations were measured by using a JASCO P 3010 polarimeter at $22 \pm 3^\circ\text{C}$. For chiral HPLC, a DAICEL CHIRALPAK AD-H column was used for 2-methyl-2,3-epoxy-1,4-naphthoquinone. Column chromatography was performed

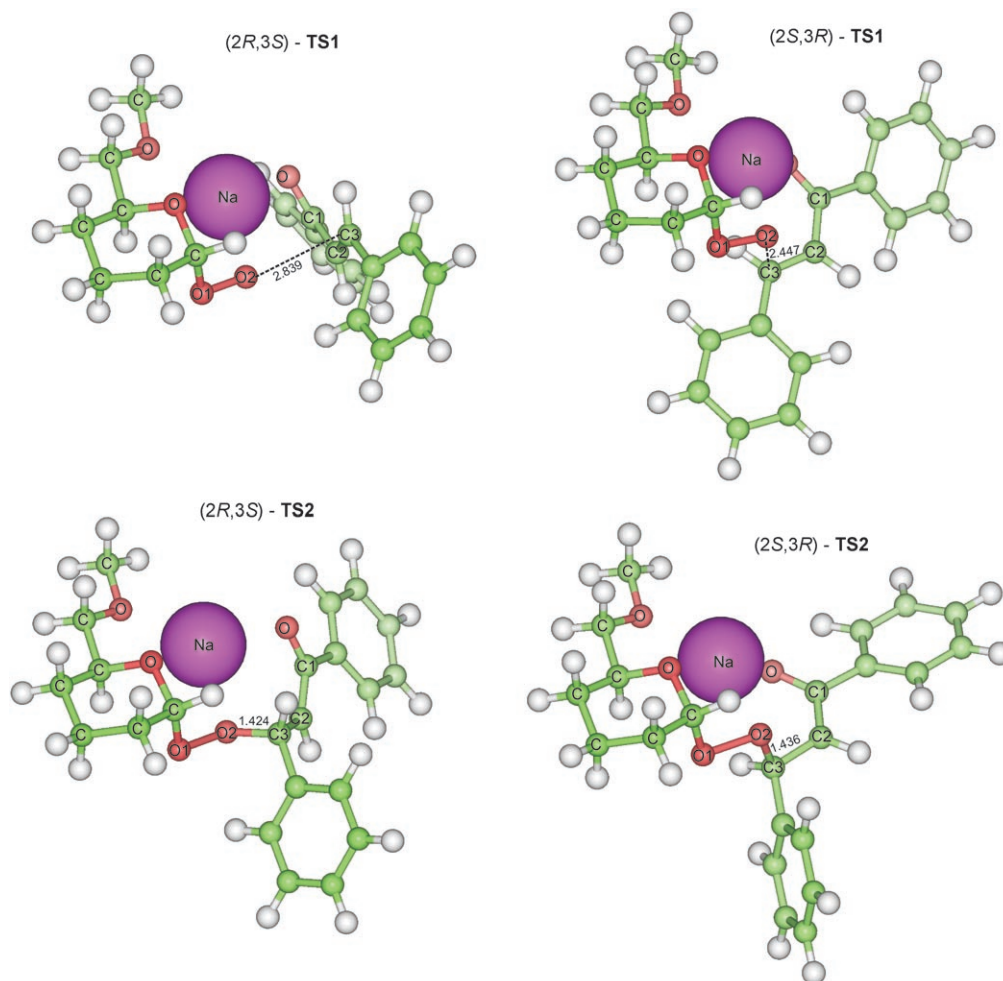


Figure 7. Geometrical representation of the diastereoselective transition states leading to the observed enantioselectivity of the epoxidation reaction in a presence of sodium calculated at the B3LYP/6-31G* level.

by using E. Merck Kiesel Gel (230–400 mesh). 6-Substituted 2-deoxy-galactosyl hydroperoxides **9–11** were obtained from the corresponding methyl glycosides by standard procedures.^[1]

All calculations were performed by using the Gaussian 03 program^[21] at the DFT level. The potential energy surfaces for two models of complex **27** with **28** were computed as a function of the $r(\text{O}2\text{--C}2)$ and $r(\text{O}2\text{--C}3)$ distances. These distances were varied by 0.05–0.3 Å increments (the smaller step was used for locations near to the transition states) within the 3.3–1.3 Å range for $r(\text{O}2\text{--C}3)$, and within the 4.2–1.3 Å range for $r(\text{O}2\text{--C}2)$. During the optimization, all geometrical parameters of reactants were optimized. As a result, each point on the potential energy surface represented by fixed values of the $r(\text{O}2\text{--C}2)$ and $r(\text{O}2\text{--C}3)$ distances have all their geometrical variables adjusted to their optimal values. Since the location of the local minima and transition barriers on the energy surface is only approximate, further optimization of the stationary points with no constraints on the $r(\text{O}2\text{--C}3)$ and $r(\text{O}2\text{--C}2)$ distances was required. The transition states were calculated by using the STQN method^[22] with QST3 options (the method requires starting geometries for reactant, product, and transition state).

Methyl 3,4-di-O-benzyl-2-deoxy-6-O-(N-ethylcarbamoyl)- α -D-lyxo-hexopyranoside: Ethyl isocyanate (0.11 mL, 1.4 mm) was added to methyl 3,4-di-O-benzyl-2-deoxy- α -D-lyxo-hexopyranoside in acetonitrile (0.7 mL, 3 mL). The reaction was stopped after 72 h (TLC analysis showed incomplete consumption of the substrate and side products appeared) and the mixture was evaporated to dryness and treated with CH_2Cl_2 . The organic layer was separated, dried over MgSO_4 , and evaporated. The crude prod-

uct was purified on a silica-gel column by using dichloromethane/acetone 25:1 v/v as the eluent to afford the corresponding 6-O-(N-ethylcarbamoyl) product (1.6 g, 52%). Solid; m.p. 73–75 °C; $[\alpha]_{\text{D}}^{20} = +45.3$ ($c = 0.98$ in CHCl_3); $^1\text{H NMR}$ (500 MHz, CDCl_3): $\delta = 4.95, 4.66$ (2 d, 2H, $J = 11.6$ Hz; PhCH_2O), 4.89 (br d, 1H, $J_{1,2a} = 3.6$ Hz; H-1), 4.62, 4.59 (2 d, 2H, $J = 12.0$ Hz; PhCH_2O), 4.56 (br s, 1H; NH), 4.22–4.12 (m, 2H; H-6a, H-6b), 3.91 (brddd, 1H; H-3), 3.86 (br t, 1H; H-5), 3.82 (br s, 1H; H-4), 3.30 (s, 3H; OCH_3), 3.24–3.14 (m, 2H; CH_2CH_3), 2.22 (ddd, 1H, $J_{2a,2b} = 12.7$, $J_{2a,3} = 12.0$, $J_{2a,1} = 3.6$ Hz; H-2a), 2.00 (dd, 1H, $J_{2b,2a} = 12.7$, $J_{2b,3} = 4.5$ Hz; H-2b), 1.12 ppm (t, 3H; CH_2CH_3); $^{13}\text{C NMR}$ (125 MHz, CDCl_3): $\delta = 155.75$ (C=O), 98.67 (C-1), 74.55 (C-4), 73.85 (PHCH_2O), 72.53 (C-3), 70.26 (PHCH_2O), 68.87 (C-5), 64.13 (C-6), 54.45 (OCH_3), 35.58 (CH_2CH_3), 30.67 (C-2), 14.95 ppm (CH_2CH_3); IR (CH_2Cl_2): $\tilde{\nu} = 3685, 3448, 2986, 1722, 1605, 1515, 1049, 896$ cm^{-1} ; HRMS (ESI): m/z : calcd for $\text{C}_{24}\text{H}_{31}\text{NO}_6\text{Na}$: 452.2044 [$M+\text{Na}$] $^+$; found: 452.2066; elemental analysis calcd (%) for $\text{C}_{24}\text{H}_{31}\text{NO}_6$: C 67.11, H 7.27, N 3.26; found: C 67.12, H 7.35, N 3.14.

Methyl 3,4-di-O-benzyl-2-deoxy-6-O-carbamoyl- α -D-lyxo-hexopyranoside: Trichloroacetyl isocyanate (0.4 mL, 3.35 mm) was added to methyl 3,4-di-O-benzyl-2-deoxy- α -D-lyxo-hexopyranoside dissolved in acetonitrile (1 mL, 2.5 mL). After the disappearance of the substrate (TLC, 1 h), the mixture was cooled to -30 °C, and benzylamine (0.5 mL, 4.5 mm) in acetonitrile (0.5 mL) was added. Subsequently, the reaction mixture was allowed to reach room temperature. The mixture was evaporated to dryness and diluted with CH_2Cl_2 and water. The water layer was separated and extracted with CH_2Cl_2 . The combined extracts were dried over

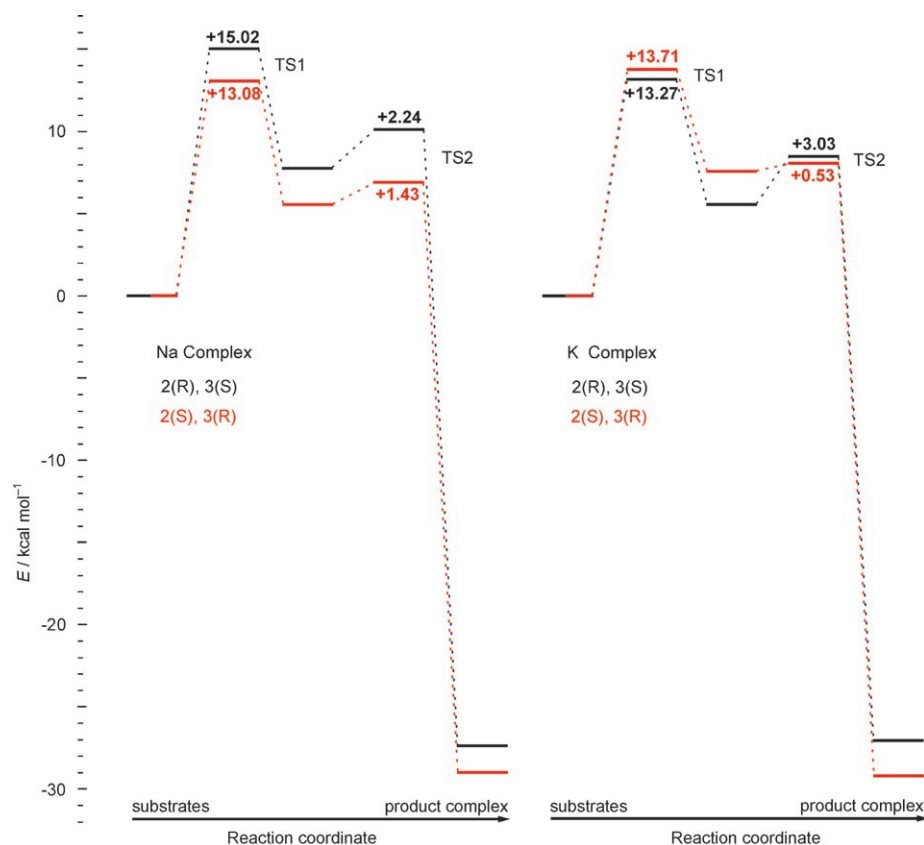


Figure 8. Schematic energetic representation [kcal mol^{-1}] of the possible reaction pathways observed in different potential energy surfaces for sodium and potassium complexes. The calculated relative free energies include the solvent effects.

MgSO_4 and evaporated. The crude product was purified on a silica-gel column by using dichloromethane/acetone 20:1 v/v as the eluent to afford the corresponding 6-*O*-carbamoyl glycoside (0.32 g, 83%). Solid; m.p. 101–103 °C; $[\alpha]_{\text{D}}^{20} = +83.0$ ($c = 0.55$ in CH_2Cl_2); $^1\text{H NMR}$ (500 MHz, CDCl_3): $\delta = 4.96, 4.66$ (2d, 2H, $J = 11.6$ Hz; PhCH_2O), 4.89 (brd, 1H; H-1), 4.62, 4.60 (2d, 2H, $J = 11.9$ Hz; PhCH_2O), 4.57 (brs, 2H; NH_2), 4.19 (dd, 1H, $J_{6a,6b} = 11.2$, $J_{6a,5} = 7.0$ Hz; H-6a), 4.16 (dd, 1H, $J_{6b,6a} = 11.2$, $J_{6b,5} = 5.4$ Hz; H-6b), 3.89 (ddd, 1H, $J_{3,2a} = 12.0$, $J_{3,2b} = 4.6$, $J_{3,4} = 2.5$ Hz; H-3), 3.87 (brt, 1H; H-5), 3.82 (brs, 1H; H-4), 3.31 (s, 3H; OCH_3), 2.22 (ddd, 1H, $J_{2a,2b} = 12.7$, $J_{2a,1} = 3.7$, $J_{2a,3} = 12.0$ Hz; H-2a), 2.01 ppm (ddd, 1H, $J_{2b,2a} = 12.7$, $J_{2b,3} = 4.6$, $J_{2b,1} = 1.2$ Hz; H-2b); $^{13}\text{C NMR}$ (125 MHz, CDCl_3): $\delta = 156.34$ (C=O), 98.96 (C-1), 74.79 (C-4), 74.12 (PHCH_2O), 72.79 (C-3), 70.55 (PHCH_2O), 69.03 (C-5), 64.88 (C-6), 54.77 (OCH_3), 30.91 ppm (C-2); IR (CH_2Cl_2): $\tilde{\nu} = 3536, 3424, 2927, 1734, 1584, 1352, 1098, 1050$ cm^{-1} ; HRMS (ESI): m/z : calcd for $\text{C}_{22}\text{H}_{27}\text{NO}_6\text{Na}$: 424.1730 [$M+\text{Na}$] $^+$; found: 424.1750; elemental analysis calcd (%) for $\text{C}_{22}\text{H}_{27}\text{NO}_6$: C 65.82, H 6.78, N 3.49; found: C 65.91, H 6.64, N 3.52.

Synthesis of hydroperoxides. General procedure: 50% H_2O_2 (14.4 mL) and concentrated H_2SO_4 (0.24 mL) were added to a solution of methyl glycoside (1.2 mm) in 1,4-dioxane (4.8 mL). The reaction was stirred at room temperature until disappearance of the substrate was complete (TLC). Subsequently, the mixture was diluted with CH_2Cl_2 (100 mL) and the organic layer was separated. The water layer was extracted with CH_2Cl_2 and the combined extracts were washed with water (caution must be taken; even a small amount of hydrogen peroxide left can cause explosion during evaporation of the solvent), dried over Na_2SO_4 , and evaporated at room temperature. The crude product was purified on a silica-gel column by using hexane/ethyl acetate 3:2 v/v as an eluent to afford the corresponding hydroperoxide.

3,4-Di-*O*-benzyl-2-deoxy- α -D-lyxo-hexopyranosyl hydroperoxide (9):

Yield: 0.35 g, 80%; solid; m.p. 89–92 °C; $[\alpha]_{\text{D}}^{20} = +62.7$ ($c = 0.6$ in CHCl_3); $^1\text{H NMR}$ (500 MHz, CDCl_3): $\delta = 9.84$ (brs, 1H; OOH), 5.43 (d, 1H, $J_{1,2a} = 4.7$ Hz; H-1), 4.93, 4.62 (2d, 2H, $J = 11.7$ Hz; PhCH_2O), 4.60, 4.56 (2d, 2H, $J = 12.0$ Hz; PhCH_2O), 3.92–3.84 (m, 2H; H-6a, H-5), 3.76 (brs, 1H; H-4), 3.73 (ddd, 1H, $J_{3,2a} = 12.3$, $J_{3,2b} = 4.7$, $J_{3,4} = 2.5$ Hz; H-3), 3.54–3.46 (m, 1H; H-6b), 2.32–2.03 (m, 1H; OH), 2.29 (ddd, 1H, $J_{2a,2b} = 13.4$, $J_{2a,3} = 12.3$, $J_{2a,1} = 4.7$ Hz; H-2a), 2.06 (dd, 1H, $J_{2b,2a} = 13.4$, $J_{2b,3} = 4.7$ Hz; H-2b); $^{13}\text{C NMR}$ (125 MHz, CDCl_3): $\delta = 102.18$ (C-1), 74.11 (C-4), 74.10 (PHCH_2O), 72.81 (C-3), 72.10 (C-5), 70.61 (PHCH_2O), 63.51 (C-6), 28.24 ppm (C-2); $^1\text{H NMR}$ (500 MHz, C_6D_6): $\delta = 10.88$ (brs, 1H; OOH), 5.47 (d, 1H, $J_{1,2a} = 4.7$ Hz; H-1), 4.88, 4.43 (2d, 2H, $J = 11.5$ Hz; PhCH_2O), 4.27, 4.22 (2d, 2H, $J = 11.9$ Hz; PhCH_2O), 4.00 (dd, 1H, $J_{6a,6b} = 11.2$, $J_{6a,5} = 8.3$ Hz; H-6a), 3.89 (m, 1H; H-5), 3.62 (ddd, 1H, $J_{3,2a} = 12.5$, $J_{3,2b} = 4.7$, $J_{3,4} = 2.5$ Hz; H-3), 3.45 (dd, 1H, $J_{6b,6a} = 11.2$, $J_{6b,5} = 3.2$ Hz; H-6b), 3.42 (brs, 1H; H-4), 2.24 (ddd, 1H, $J_{2a,2b} = 13.3$, $J_{2a,3} = 12.5$, $J_{2a,1} = 4.7$ Hz; H-2a), 1.92 (ddd, 1H, $J_{2b,2a} = 13.3$, $J_{2b,3} = 4.7$, $J_{2b,1} = 1.2$ Hz; H-2b); $^{13}\text{C NMR}$ (125 MHz, C_6D_6): $\delta = 102.67$ (C-1), 74.73 (C-4), 74.44 (PHCH_2O), 73.97 (C-3), 72.82 (C-5), 70.51 (PHCH_2O), 64.04 (C-6), 28.62 ppm (C-2); IR (film): $\tilde{\nu} = 3325, 1454, 1362, 1112,$

1039, 1028, 737, 698 cm^{-1} ; HRMS (ESI): m/z : calcd for $\text{C}_{20}\text{H}_{24}\text{O}_6\text{Na}$: 383.1465; found: 383.1448 [$M+\text{Na}$] $^+$; elemental analysis calcd (%) for $\text{C}_{20}\text{H}_{24}\text{O}_6$: C 66.65, H 6.71; found: C 66.76, H 6.78.

3,4-Di-*O*-benzyl-2-deoxy-6-*O*-carbamoyl- α -D-lyxo-hexopyranosyl hydroperoxide (10):

Yield: 0.38 g, 79%; solid; m.p. 144–146 °C; $[\alpha]_{\text{D}}^{20} = +59.4$ ($c = 0.6$ in CH_2Cl_2); $^1\text{H NMR}$ (500 MHz, CDCl_3): $\delta = 9.62$ (s, 1H; OOH), 5.41 (d, 1H, $J_{1,2a} = 4.4$ Hz; H-1), 4.96, 4.65 (2d, 2H, $J = 11.5$ Hz; PhCH_2O), 4.76 (brs, 2H; NH_2), 4.61, 4.57 (2d, 2H, $J = 12.0$ Hz; PhCH_2O), 4.26 (dd, 1H, $J_{6a,6b} = 11.3$, $J_{6a,5} = 6.8$ Hz; H-6a), 4.13 (dd, 1H, $J_{6b,6a} = 11.3$, $J_{6b,5} = 5.8$ Hz; H-6b), 4.02 (m, 1H; H-5), 3.81 (brs, 1H; H-4), 3.74 (ddd, 1H, $J_{3,2a} = 12.4$, $J_{3,2b} = 4.6$, $J_{3,4} = 2.4$ Hz; H-3), 2.29 (ddd, 1H, $J_{2a,2b} = 13.4$, $J_{2a,3} = 12.4$, $J_{2a,1} = 4.4$ Hz; H-2a), 2.04 ppm (dd, 1H, $J_{2b,2a} = 13.4$, $J_{2b,3} = 4.6$ Hz; H-2b); $^{13}\text{C NMR}$ (125 MHz, CDCl_3): $\delta = 156.87$ (C=O), 101.88 (C-1), 74.26 (PHCH_2O), 73.95 (C-4), 72.25 (C-3), 70.56 (PHCH_2O), 69.70 (C-5), 64.31 (C-6), 28.09 ppm (C-2); $^1\text{H NMR}$ (500 MHz, C_6D_6): $\delta = 9.05$ (s, 1H; OOH), 5.44 (brd, 1H, $J_{1,2a} = 4.4$ Hz; H-1), 5.03 (d, 1H; PhCH_2O), 4.62 (d, 1H; PhCH_2O), 4.26 (dd, 1H, $J_{6a,6b} = 11.1$, $J_{6a,5} = 6.8$ Hz; H-6a), 4.43 (dd, 1H, $J_{6b,6a} = 11.1$, $J_{6b,5} = 5.7$ Hz; H-6b), 4.33–4.26 (m, 2H; PhCH_2O), 4.17 (m, 1H; H-5), 3.87 (brs, 2H; NH_2), 3.70–3.63 (m, 2H; H-4, H-3), 2.33 (ddd, 1H, $J_{2a,2b} = 13.3$, $J_{2a,3} = 12.2$, $J_{2a,1} = 4.4$ Hz; H-2a), 1.93 (dd, 1H, $J_{2b,2a} = 13.3$, $J_{2b,3} = 4.6$ Hz; H-2b); IR (CH_2Cl_2): $\tilde{\nu} = 3532, 3423, 2990, 1735, 1425, 1356, 1111, 1053, 897$ cm^{-1} ; HRMS (ESI): m/z : calcd for $\text{C}_{21}\text{H}_{25}\text{NO}_7\text{Na}$: 426.1523 [$M+\text{Na}$] $^+$; found: 426.1537; elemental analysis calcd (%) for $\text{C}_{21}\text{H}_{25}\text{NO}_7$: C 62.52, H 6.25, N 3.47; found: C 62.41, H 6.16, N 3.33.

3,4-Di-*O*-benzyl-2-deoxy-6-*O*-(*N*-ethylcarbamoyl)- α -D-lyxo-hexopyranosyl hydroperoxide (11):

Yield: (0.37 g, 72%); solid; m.p. 112–114 °C; $[\alpha]_{\text{D}}^{20} = +54.9$ ($c = 0.35$ in CH_2Cl_2); $^1\text{H NMR}$ (500 MHz, CDCl_3): $\delta = 8.95$ (brs, 1H; OOH), 5.42 (d, 1H, $J_{1,2a} = 4.7$ Hz; H-1), 4.96, 4.66 (2d, 2H, $J = 11.5$ Hz; PhCH_2O), 4.63 (brs, 1H; NH), 4.60, 4.57 (2d, 2H, $J = 12.0$ Hz;

PhCH₂O), 4.27–3.99 (m, 3H; H-6a, H-6b, H-5), 3.81 (m, 1H; H-4), 3.74 (ddd, 1H, $J_{3,2a}=12.3$, $J_{3,2b}=4.7$, $J_{3,4}=2.4$ Hz; H-3), 3.24–3.14 (brm, 2H; CH₂CH₃), 2.30 (ddd, 1H, $J_{2a,2b}=13.5$, $J_{2a,3}=12.3$, $J_{2a,1}=4.7$ Hz; H-2a), 2.04 (dd, 1H, $J_{2b,2a}=13.5$, $J_{2b,3}=4.7$ Hz; H-2b), 1.12 ppm (t, 3H; CH₂CH₃); ¹³C NMR (125 MHz, CDCl₃): δ 101.88 (C-1), 74.26 (PHCH₂O), 74.05 (C-4), 72.30 (C-3), 70.58 (PHCH₂O), 69.84 (C-5), 64.00 (C-6), 35.93 (CH₂CH₃), 28.08 (C-2), 15.12 ppm (CH₂CH₃); ¹H NMR (500 MHz, C₆D₆): δ = 9.30 (brs, 1H; OOH), 5.39 (brm, 1H; H-1), 4.96, 4.57 (2d, 2H, $J=11.3$ Hz; PhCH₂O), 4.56–4.50 (m, 1H; H-6a), 4.40 (dd, 1H, $J_{6b,6a}=11.2$, $J_{6b,5}=6.0$ Hz; H-6b), 4.23, 4.19 (2d, 2H, $J=12.0$ Hz; PhCH₂O), 4.18 (m, 1H; H-5), 4.10 (brs, 1H; NH), 3.65 (m, 1H; H-4), 3.58 (ddd, 1H, $J_{3,2a}=12.3$, $J_{3,2b}=4.9$, $J_{3,4}=2.4$ Hz; H-3), 2.92–2.83 (m, 2H; CH₂CH₃), 2.24 (ddd, 1H, $J_{2a,2b}=13.3$, $J_{2a,3}=12.3$, $J_{2a,1}=4.6$ Hz; H-2a), 2.04 (dd, 1H, $J_{2b,2a}=13.3$, $J_{2b,3}=4.9$ Hz; H-2b), 0.73 ppm (t, 3H; CH₂CH₃); ¹³C NMR (125 MHz, C₆D₆): δ = 156.51 (C=O), 102.17 (C-1), 74.76 (C-4), 74.64 (PHCH₂O), 73.42 (C-3), 70.47 (PHCH₂O), 70.18 (C-5), 64.39 (C-6), 35.97 (CH₂CH₃), 28.45 (C-2), 15.07 ppm (CH₂CH₃); IR (CH₂Cl₂): $\tilde{\nu}=3446, 2930, 1723, 1517, 1454, 1360, 1112, 1028$ cm⁻¹; HRMS (ESI): m/z : calcd for C₂₃H₃₀NO₇: 432.2017 [$M+H$]⁺; found: 432.2035; elemental analysis calcd (%) for C₂₃H₃₀NO₇: C 64.02, H 6.77, N 3.25; found: C 63.97, H 6.68, N 3.14.

Epoxidation of enones. General procedure: Freshly powdered NaOH (0.224 mm) was added under argon to a solution of hydroperoxide (0.224 mm) in anhydrous toluene (31 mL), and after 10 min of vigorous stirring, a solution of enone (0.149 mm) in toluene (21 mL) was introduced by syringe. The reaction was stirred at room temperature until disappearance of the substrate was complete (TLC). Subsequently, the mixture was diluted with CH₂Cl₂ (50 mL) and the organic layer was separated. The water layer was extracted once with CH₂Cl₂ and the combined extracts were washed with water, dried over Na₂SO₄, and evaporated. The crude product was purified on a silica-gel column by using hexane/ethyl acetate 9:1 v/v as the eluent to afford the corresponding epoxide.

Trans-(2S,3R)-2,3-epoxy-1,3-diphenylpropane-1-one (23): Yield: 0.032 g, 97%; [α]_D²⁰ = +190 ($c=1.08$ in CH₂Cl₂); ¹H NMR (500 MHz, CDCl₃): δ = 8.02 (m, 2H; Ph), 7.62 (m, 1H; Ph), 7.49 (m, 2H; Ph), 7.39 (m, 5H; Ph), 4.29 (d, 1H, $J=1.8$ Hz), 4.08 ppm (d, 1H, $J=1.8$ Hz); ¹³C NMR (125 MHz, CDCl₃): δ = 193.08 (C=O), 135.52, 133.97, 129.05, 128.88, 128.78, 128.37, 125.80, 61.05, 59.36 ppm; HRMS (EI): m/z : calcd for C₁₅H₁₂O₂: 224.0837 [M]⁺; found: 224.0830; UV (CH₃CN): λ_{max} (ϵ) = 191.0 (55627), 247.3 nm (14593 mol⁻¹dm³cm⁻¹); CD (CH₃CN): $\Delta\epsilon_{325} = 2.8$, $\Delta\epsilon_{257} = 5.7$, $\Delta\epsilon_{235} = -7.5$, $\Delta\epsilon_{199} = 11.5$ mol⁻¹dm³cm⁻¹ ($c=0.3 \times 10^{-3}$ M, 90.5% ee); HPLC (DAICEL CHIRALPAK AD-H: flow rate = 1.0 mL min⁻¹, $\lambda=254$ nm, hexane/*i*PrOH 93:7, retention time = 14.1 (2S,3R), 15.1 min (2R,3S).

Trans-(2S,3R)-2,3-epoxy-1,4-diphenylbutane-1,4-one (24): Yield: 0.039 g, 98%; [α]_D²⁰ = +110 ($c=0.57$ in CHCl₃); ¹H NMR (500 MHz, CDCl₃): δ = 8.06 (m, 4H; Ph), 7.65 (m, 2H; Ph), 7.52 (m, 4H; Ph), 4.49 ppm (s, 2H; 2 × CH); ¹³C NMR (125 MHz, CDCl₃): δ = 192.15 (C=O), 135.07, 134.46, 129.04, 128.64, 56.41 ppm; HRMS (ESI): m/z : calcd for C₁₆H₁₂O₃Na: 275.0679 [$M+Na$]⁺; found: 275.0673; UV (CH₃CN): λ_{max} (ϵ) = 193.9 (44007), 250.6 nm (23822 mol⁻¹dm³cm⁻¹); CD (CH₃CN): $\Delta\epsilon_{330} = 3.3$, $\Delta\epsilon_{261} = -7.7$, $\Delta\epsilon_{242} = 2.3$, $\Delta\epsilon_{218} = -3.7$, $\Delta\epsilon_{204} = 5.9$ ($c=0.27 \times 10^{-3}$ M, 78% ee); HPLC (DAICEL CHIRALCEL OD-H): flow rate = 1.0 mL min⁻¹, $\lambda=254$ nm, hexane/*i*PrOH 9:1, retention time = 15.4 min (2R,3R), 17.6 min (2S,3S).

Trans-(1R,2S)-1,2-epoxy-4-methyl-1-phenyl-pentane-3-one (25): Yield: 0.028 g, 98%; [α]_D²⁰ = +130.5 ($c=0.30$ in CHCl₃); ¹H NMR (500 MHz, CDCl₃): δ = 7.36 (m, 3H; Ph), 7.29 (m, 2H; Ph), 3.92 (d, 1H, $J=1.9$ Hz; CH), 3.60 (d, 1H, $J=1.9$ Hz; CH), 2.82 (sept, 1H; CH(CH₃)₂), 1.17 ppm (t, 6H; CH(CH₃)₂); ¹³C NMR (125 MHz, CDCl₃): δ = 208.64 (C=O), 135.37, 128.93, 128.68, 125.67, 61.86, 58.38, 36.86, 18.05, 17.29 ppm; HRMS (EI): m/z : calcd for C₁₂H₁₄O₂: 190.0994 [M]⁺; found: 190.1002; UV (*i*PrOH): λ_{max} (ϵ) = 224.8 (11161 mol⁻¹dm³cm⁻¹); CD (*i*PrOH): $\Delta\epsilon_{287} = 0.7$, $\Delta\epsilon_{226} = 4.1$, $\Delta\epsilon_{207} = 0.9$ mol⁻¹dm³cm⁻¹ ($c=0.98 \times 10^{-3}$ M, 87% ee); HPLC (DAICEL CHIRALPAK AS-H): flow rate = 1.0 mL min⁻¹, $\lambda=225$ nm, hexane/*i*PrOH 95:5, retention time = 6.9 min (2S,3R), 9.2 min (2R,3S).

Acknowledgements

This work was supported by the State Committee for Scientific Research (grant no. 3 T09A 024 28 and by grants from the Slovak Research and Development Agency (no. APVV-51-004204 and the Slovak Grant Agency VEGA (no. 2/6129/26).

- [1] W. Košník, A. Stachulski, M. Chmielewski, *Tetrahedron: Asymmetry* **2005**, *16*, 1975–1981; Corrigendum: *Tetrahedron: Asymmetry* **2006**, *17*, 313.
- [2] a) W. Adam, R. T. Fell, U. Hoch, C. R. Saha-Möllner, P. Schreier, *Tetrahedron: Asymmetry* **1995**, *6*, 1047–1050; b) W. Adam, U. Hoch, M. Lazarus, C. R. Saha-Möllner, P. Schreier, *J. Am. Chem. Soc.* **1995**, *117*, 11898–11901; c) W. Adam, P. B. Rao, H.-G. Degen, C. R. Saha-Möllner, *J. Am. Chem. Soc.* **2000**, *122*, 5654–5655; d) W. Adam, P. B. Rao, H.-G. Degen, C. R. Saha-Möllner, *Eur. J. Org. Chem.* **2002**, 630–639.
- [3] A. Lattanzi, M. Cocilova, P. Iannece, A. Scettri, *Tetrahedron: Asymmetry* **2004**, *15*, 3751–3755.
- [4] a) C. L. Dwyer, C. D. Gill, O. Ichihawa, R. J. K. Taylor, *Synlett* **2000**, 704–706; b) A. Bundu, N. G. Berry, C. D. Gill, C. L. Dwyer, A. V. Stachulski, R. J. K. Taylor, J. Whittall, *Tetrahedron: Asymmetry* **2005**, *16*, 283–293.
- [5] a) H. J. Hamann, E. Höft, J. Liebscher, in *Peroxide Chemistry, Mechanistic and Preparative Aspects of Oxygen Transfer* (Ed.: W. Adam), Wiley-VCH, Weinheim, **2000**, pp. 381–405; b) F. G. Gelacha, *Chem. Rev.* **2007**, *107*, 3338–3361; c) K. Žmitek, M. Zupan, J. Iskra, *Org. Biomol. Chem.* **2007**, *5*, 3895–3908; d) C. Lauret, S. M. Roberts, *Al-drichimica Acta* **2002**, *35*, 47–51.
- [6] M. Chmielewski, J. Jurczak, S. Maciejewski, *Carbohydr. Res.* **1987**, *165*, 111–115.
- [7] a) H. J. Hamann, E. Höft, D. Mostowicz, A. Mishnev, Z. Urbańczyk-Lipkowska, M. Chmielewski, *Tetrahedron* **1997**, *53*, 185–192; b) D. Mostowicz, M. Jurczak, H. J. Hamann, E. Höft, M. Chmielewski, *Eur. J. Org. Chem.* **1998**, 2617–2621.
- [8] M. Chmielewski, *Polish J. Chem.* **1980**, *54*, 1913–1921.
- [9] P. A. Bentley, J. F. Bickley, S. M. Roberts, A. Steiner, *Tetrahedron Lett.* **2001**, *42*, 3741–3743.
- [10] a) D. Enders, Jiqun Zhu, L. Kramps, *Liebigs Ann./Recl.* **1997**, 1101–1113; b) S. Watanabe, T. Arai, H. Sasaki, M. Bougauchi, M. Shibasaki, *J. Org. Chem.* **1998**, *63*, 8090–8091; c) M. J. Porter, J. Skidmore, *Chem. Commun.* **2000**, 1215–1225.
- [11] W. Košník, W. Bocian, L. Kozerski, M. Chmielewski, I. Tvaroška, *Carbohydr. Res.* in press.
- [12] D. V. Deubel, G. Frenking, P. Gisdakis, W. A. Herrmann, N. Rösch, J. Sundermeyer, *Acc. Chem. Res.* **2004**, *37*, 645–652.
- [13] R. D. Bach, M. N. Glukhovtsev, C. Gonzales, *J. Am. Chem. Soc.* **1998**, *120*, 9902–9910.
- [14] R. D. Bach, O. Dmitrenko, W. Adam, S. Schambony, *J. Am. Chem. Soc.* **2003**, *125*, 924–934.
- [15] J. Sundermeyer, *Angew. Chem.* **1993**, *105*, 1195–1197; *Angew. Chem. Int. Ed. Engl.* **1993**, *32*, 1144–1146.
- [16] K. B. Sharpless, J. M. Townsend, D. R. Williams, *J. Am. Chem. Soc.* **1972**, *94*, 295–296.
- [17] E. N. Jacobsen, *Catalytic Asymmetric Synthesis* (Eds. I. Ojima), VCH, New York, **1993**, pp. 159–202.
- [18] H. Mimoun, I. Sere de Roch, L. Sajus, *Tetrahedron* **1970**, *26*, 37–50.
- [19] C. A. Bunton, G. J. Minkoff, *J. Chem. Soc.* **1949**, 665–670.
- [20] C. F. Christian, T. Takeya, M. J. Szymanski, D. A. Singleton, *J. Org. Chem.* **2007**, *72*, 6183–6189.
- [21] Gaussian 03, Revision D.02, M. J. Frisch, G. W. Trucks, H. B. Schlegel, G. E. Scuseria, M. A. Robb, J. R. Cheeseman, J. A. Montgomery, Jr., T. Vreven, K. N. Kudin, J. C. Burant, J. M. Millam, S. S. Iyengar, J. Tomasi, V. Barone, B. Mennucci, M. Cossi, G. Scalmani, N. Rega, G. A. Petersson, H. Nakatsuji, M. Hada, M. Ehara, K. Toyota, R. Fukuda, J. Hasegawa, M. Ishida, T. Nakajima, Y. Honda, O. Kitao, H. Nakai, M. Klene, X. Li, J. E. Knox, H. P. Hratchian, J. B. Cross,

V. Bakken, C. Adamo, J. Jaramillo, R. Gomperts, R. E. Stratmann, O. Yazyev, A. J. Austin, R. Cammi, C. Pomelli, J. W. Ochterski, P. Y. Ayala, K. Morokuma, G. A. Voth, P. Salvador, J. J. Dannenberg, V. G. Zakrzewski, S. Dapprich, A. D. Daniels, M. C. Strain, O. Farkas, D. K. Malick, A. D. Rabuck, K. Raghavachari, J. B. Foresman, J. V. Ortiz, Q. Cui, A. G. Baboul, S. Clifford, J. Cioslowski, B. B. Stefanov, G. Liu, A. Liashenko, P. Piskorz, I. Komaromi, R. L. Martin, D. J. Fox, T. Keith, M. A. Al-Laham, C. Y. Peng, A. Na-

nayakkara, M. Challacombe, P. M. W. Gill, B. Johnson, W. Chen, M. W. Wong, C. Gonzalez, and J. A. Pople, Gaussian, Inc., Wallingford CT, **2004**.
[22] Standard method within the Gaussian program.

Received: January 10, 2008
Published online: May 26, 2008